

Frequency-domain elastic waveform inversion using weighting factors related to source-deconvolved residuals

Ju-Won Oh¹, Dong-Joo Min¹, and Felix J. Herrmann²

(¹ Seoul National University and ² the University of British Columbia)

Summary

One of the limitations in seismic waveform inversion is that inversion results are very sensitive to initial guesses, which may be because the gradients computed at each frequency are not properly weighted depending on given models. Analyzing the conventional waveform inversion algorithms using the pseudo-Hessian matrix as a pre-conditioner shows that the gradients do not properly describe the feature of given models or high- and low-end frequencies do not contribute the model parameter updates due to banded spectra of source wavelet. For a better waveform inversion algorithm, we propose applying weighting factors to gradients computed at each frequency. The weighting factors are designed using the source-deconvolved back-propagated wavefields. Numerical results for the SEG/EAGE salt model show that the weighting method improves gradient images and its inversion results are compatible with true velocities even with poorly estimated initial guesses.

Introduction

Seismic waveform inversion is a useful method to estimate subsurface physical properties from seismic data recorded at the surface. Although seismic waveform inversion has been extensively studied over more than two decades, it still suffers from several problems. One of them is that it is hard to obtain global minimum solutions, when the initial guess is poorly estimated. Some geophysicists have used seismic traveltime tomography results for initial guesses and the Laplace-domain waveform inversion also has proven to present good initial guesses (Shin and Cha, 2008). Bunks et al. (1995) proposed using the multi-scale method in which waveform inversion is performed beginning with only low frequency data and moving towards high frequencies. The multi-scale method helps us obtain solutions close to global minimum. This concept has also been applied in the frequency domain, and Sirgue and Pratt (2004) and Lin and Herrmann (2007) improved its computational efficiency. On the other hand, as an alternative to the multi-scale method, Lazaratos et al. (2011) proposed introducing the spectral shaping filter based on well log data.

In this study, we analyze the reason why waveform inversion easily gets stuck in local minima and propose a weighting method to overcome the limitation. Our method is based on the principle that the gradients obtained at each frequency have different spatial resolution and thus contribute to recovering different-wavelength structures. For example, the gradients obtained at low frequencies will be more important than those at high frequencies to invert long-wavelength structures such as salt structures. Our weighting method is designed to control the degree of contribution of gradients obtained at each frequency to model parameter updates. The weights are determined by the source-deconvolved residuals, which reflect parameter deviations between true and inverted models at the each iteration.

Inverse theory

In waveform inversion using the l_2 norm, the objective function can be expressed by

$$E(\mathbf{p}) = \sum_{\omega} \sum_s \frac{1}{2} \|\mathbf{u}_s(\omega, \mathbf{p}) - \mathbf{d}_s(\omega)\|_2^2, \quad (1)$$

where \mathbf{d}_s and \mathbf{u}_s are the field and modelled data, respectively, \mathbf{p} indicates the model parameter, and ω and s denote the angular frequency and the source position, respectively. The model parameter updates can be obtained by computing the gradient direction of objective function and the gradient can be calculated using the adjoint operator. In that case, the gradient with respect to the entire model parameter can be written as

$$\nabla_{\mathbf{p}} E = \sum_{\omega} \sum_s \text{Re}\{(\mathbf{F}_s^v)^T (\mathbf{S}^{-1})^T (\mathbf{u}_s - \mathbf{d}_s)^*\}, \quad (2)$$

where the superscripts T and $*$ denote the transpose and the complex conjugate, respectively and \mathbf{F}_s^v is the virtual source matrix used to compute partial derivative wavefields. The last two terms indicate the back-propagation of residuals (Pratt et al. 1998). The model parameters can be updated using

$$\delta \mathbf{p}^{(l)} = \mathbf{p}^{(l+1)} - \mathbf{p}^{(l)} = -\alpha \nabla_{\mathbf{p}} E, \quad (3)$$

where α is the step length. In the gradient method, it is hard to recover the deeper parts of subsurface model because the seismic sources are located at the surface and the gradients near the surface are much larger than those of the deeper parts. Therefore, we usually use the Hessian matrix as a preconditioner.

In this study, we use the diagonal of the pseudo Hessian matrix (Shin et al. 2001) to scale the gradients and apply the conjugate gradient method to accelerate the convergence rate. We also invert source wavelet during inversion process.

Weighting method

According to Jang et al. (2009), we can use the pseudo-Hessian matrix inside or outside the frequency loop to scale the gradient. The former, which scales the gradient inside the frequency loop, has the advantage that each frequency component equally contributes to model parameter updates because

the source spectra included in both the gradient (i.e., numerator) and the pseudo-Hessian matrix (i.e., denominator) can be removed through cancellation. On the other hand, in the second method, which scales the gradient outside the frequency loop, the source spectra act as weighting functions and play a role in restricting the contribution of the low- and high-end frequency components to model parameter updates.

In the first method, because the pseudo-Hessian matrix is applied inside the frequency loop, it can also have an effect of weighting the gradients obtained at each frequency, but its effect does not coincide with the general inverse theory. In other words, model parameter updates are not directly affected by the gradients themselves. For this reason the first method has been used by normalizing the gradient (scaled by the pseudo Hessian matrix) by its maximum value at each frequency, which can be expressed by

$$\delta \mathbf{p} = \sum_{\omega} \frac{\delta \mathbf{p}_{\omega}}{|\delta \mathbf{p}_{\omega}|_{\max}} \text{ with } \delta \mathbf{p}_{\omega} = \frac{\sum_s \text{Re}[(\mathbf{F}_s^v)^T (\mathbf{S}^{-1})^T (\mathbf{u}_s - \mathbf{d}_s)^*]}{\sum_s [(\mathbf{F}_s^v)^T (\mathbf{F}_s^v)^* + \beta \mathbf{I}]}, \quad (4)$$

where β is a damping factor. On the other hand, the second method conforms to the general inverse theory, because the gradients are scaled by the same value (i.e., the final pseudo-Hessian matrix obtained by summing the pseudo-Hessian matrices at each frequency). In this case, if we could remove the source spectra properly, the gradient $(\mathbf{F}_s^v)^T (\mathbf{S}^{-1})^T (\mathbf{u}_s - \mathbf{d}_s)^*$ at each frequency will contribute to recovering different-wavelength structures. With the source wavelet deconvolved, the last two terms indicate the source-deconvolved back-propagated wavefield. This source-deconvolved back-propagated wavefield can be important in the inverse problem, because their relative amplitudes are controlled by the deconvolved residual vectors that result from discrepancies between true and inverted models at every iteration step. However, in practice, it is not easy to remove only the source wavelet not deforming the characteristic of the gradient.

In this study, we design a weighting method to overcome the limitation of the first method. In this case, the model parameter update in equation (4) can be rewritten by

$$\delta \mathbf{p} = \sum_{\omega} \gamma_{\omega} \frac{\delta \mathbf{p}_{\omega}}{|\delta \mathbf{p}_{\omega}|_{\max}} \text{ with } \gamma_{\omega} = \frac{\sum_{i=1}^{np} |\tilde{v}_i|}{np}, \quad (5)$$

where np is the number of nodal points, and \tilde{v}_i is the deconvolved back-propagated wavefield. The source-deconvolved back-propagated wavefield is obtained by removing source wavelet from residuals based on the source wavelet estimated at the each iteration. For the weighting factor, we only use the average of wavefields recorded at all the nodal point by backpropagating the residuals measured at the receivers when the source is located in the middle of the surface in order to avoid the complexity caused by combining numerous data for whole shot gathers

Numerical Examples for the SEG/EAGE salt model

The salt model is one of the challenging models in elastic waveform inversion. When the initial velocity structures are not close to the true model, the high velocity of the salt body and the low velocity zone below the salt body are not properly inverted even though we use the frequency-selection strategy beginning with very low frequencies in our experience. We need to examine if the weighting method can enhance the inversion results compared to the conventional method (corresponding to the first method that scale the gradient by the pseudo Hessian matrix inside the frequency loop), when the initial models are poorly estimated. Figure 1 shows a 2D section of the SEG/EAGE salt model (AA' line). The S-wave velocities are generated assuming Poisson's ratio to be fixed at 0.25 and parameters for the inversion are listed in Table 1.

Table 1 Parameters used for inversion.

Dimension	No. of shots	No. of receivers	Interval of shots	Interval of receivers	Recording time	Maximum Frequency	Minimum Frequency
15.6 km × 4.2 km	390	781	0.04 km	0.02 km	6 sec	10 Hz	0.167 Hz

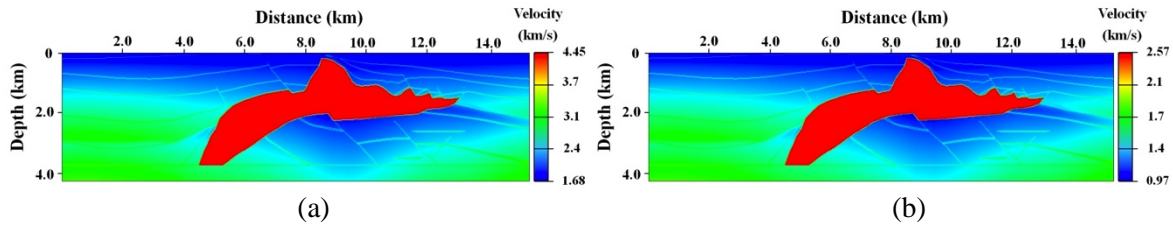


Figure 1 The SEG/EAGE salt model: (a) P- and (b) S-wave velocities.

In our waveform inversion, we use the finite-element method based on Galerkin's method for forward simulations. We only update Lamé constants independently assuming that the density is constant at 2.0 g/cm^3 for the entire model. To generate the source wavelet, we use the first derivative of Gaussian function with a cutoff frequency of 10 Hz. We use all the frequencies ranging from 0.167 to 10 Hz with an interval of 0.167 Hz under the assumption that the low frequency data can be obtained from OBS data as Plessix (2009) addressed. As initial models, the P-wave velocities gradually increase from 1.5 to 3.06 km/s and the S-wave velocities are constructed from P-wave velocities and Poisson's ratio fixed at 0.25.

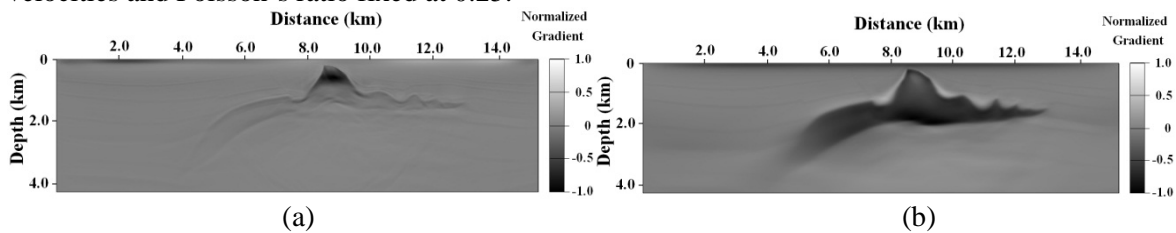


Figure 2 Gradient images for μ obtained at the 300th iteration by the (a) conventional and (b) weighting methods.

Figure 2 shows gradient images for μ obtained by the conventional and weighting methods at the 300th iteration. In the weighting method, the gradient image properly describes long-wavelength structure of the salt body, which may indicate that the gradients obtained at low frequencies are more weighted than those at high frequencies. In contrast, the gradient image obtained by the conventional method is not compatible with the true model. Figures 3 and 4 show the P-wave velocity models inverted by the conventional and weighting methods at the 700th iteration. We observe that the salt body recovered by the conventional method is thinner than that of the true model and that the velocities below the salt body are higher than those of the original version due to the poor gradients (Figure 2a) as reported by previous studies. On the other hand, the inverted P-wave velocities using the weighting method (Figures 3b and 4b) agree well with the true velocities. Although we do not show the inversion results for S-wave velocities, they show similar aspects to P-wave velocities.

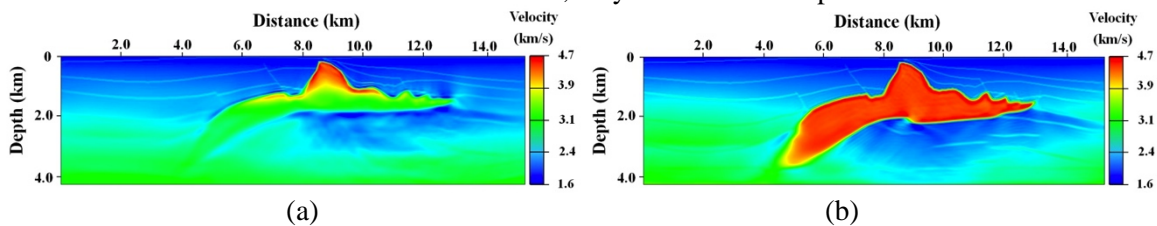


Figure 3 P-wave velocity structures inverted by the (a) conventional and (b) weighting methods.

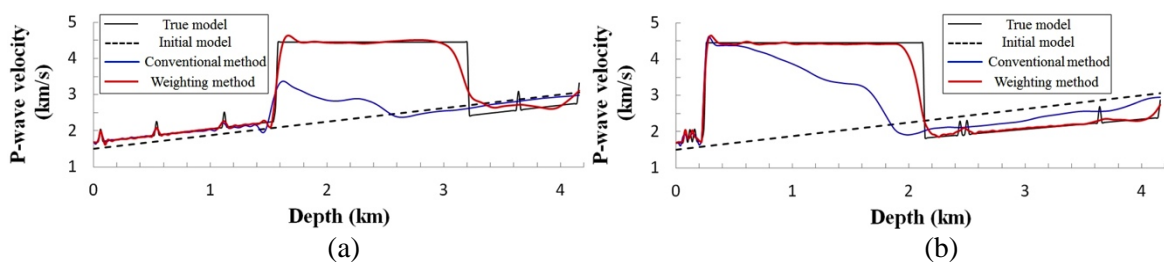


Figure 4 Depth profiles at distances of (a) 6 km and (b) 9 km of P-wave velocities shown in Figure 3.

In Figure 5a, the RMS errors of source-deconvolved residuals for the weighting method are much lower than those of the conventional method over frequencies, in particular at low frequencies. Figure 5b shows simulated data for the inverted velocity models obtained by the conventional and weighting methods. To consider all of the data recorded for the entire shot, receiver and frequency, the amplitudes of wavefields recorded at all of the receivers for all of the sources are summed at each frequency after the source spectra are removed. The modeled data obtained by the weighting method are consistent with the true data in contrast with those by the conventional method.

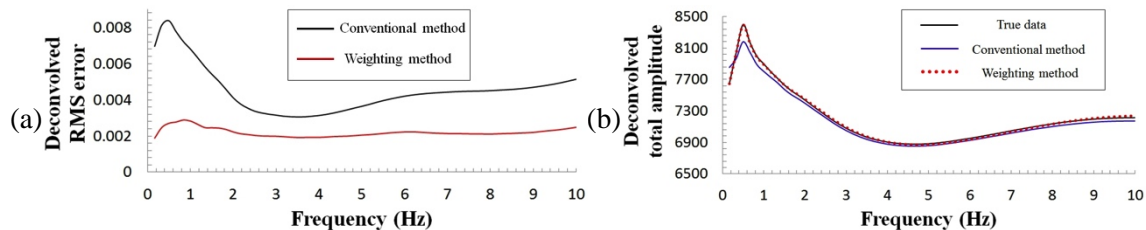


Figure 5(a) RMS errors of deconvolved residuals at the 200th iteration and (b) summed amplitudes of true data and simulated data.

Conclusions

We proposed the weighting method for frequency-domain elastic waveform inversion to alleviate the sensitivity of inversion results to initial guesses. The weighting factors need to be designed to make the gradient directions reflect the distribution of deconvolved residuals resulting from differences between the true and inverted models. We used the deconvolved back-propagated wavefields for the weighting factors. Numerical results for the SEG/EAGE salt model demonstrate that while the conventional method fails in properly recovering the salt body and the low velocity zone below it, the weighting method gives inversion results compatible with the true velocities without additional computational costs.

Acknowledgements

This work was financially supported by the BK 21 project, the Basic Science Research Program through the NRF funded by the MEST (2010-0006155), the Energy Efficiency & Resources of the KETEP grant funded by the MKL (No. 2010T100200133), and the CO₂ project of KORDI.

References

- Bunks, C., Saleck, F.M., Zaleski, S. and Chavent, G. [1995] Multiscale seismic waveform inversion. *Geophysics*, **60**, 1457-1473.
- Jang, U., Min, D.J. and Shin, C. [2009] Comparison of scaling methods for waveform inversion. *Geophysical Prospecting*, **57**, 49-59.
- Lazaratos, S., Chikichev, I. and Wang, K. [2011] Improved the convergence rate of full waveform inversion using spectral shaping. *Expanded Abstracts of the 81th International Annual Meeting. SEG*, San Antonio, 2428-2432.
- Plessix, R. [2009] Three-dimensional frequency-domain full-waveform inversion with an iterative solver. *Geophysics*, **74**, WCC149-WCC157.
- Pratt, R.G., Shin, C. and Hicks, G.J., [1998] Gauss-Newton and full Newton methods in frequency-space seismic waveform inversion. *Geophys. J. Int.*, **133**, 341-362.
- Shin, C., Jang, S. and Min, D.J. [2001] Improved amplitude preservation for prestack depth migration by inverse scattering theory. *Geophysical Prospecting*, **49**, 592-606.
- Shin, C. and Cha, Y.H. [2008] Waveform inversion in the Laplace domain. *Geophys. J. Int.*, **17**, 922-931.
- Sirgue, L. and Pratt, R.G. [2004] Efficient waveform inversion and imaging: A strategy for selecting temporal frequencies. *Geophysics*, **69**, 231-248.
- Lin, T.T.Y. and Herrmann, F. J. [2007] Compressed wavefield extrapolation. *Geophysics*, **72**, SM77-SM93.